

---

# Learning-Zone Energy: Online Data Selection for Efficient RL Post-Training

---

<sup>1</sup>Peng Cui\*, <sup>2</sup>Boyao Yang\*, <sup>1</sup>Jun Zhu<sup>†</sup>

<sup>1</sup> Dept. of Comp. Sci. & Tech., Institute for AI, BNRist Center,  
Tsinghua-Bosch Joint ML Center, THBI Lab, Tsinghua University, Beijing 100084, China

<sup>2</sup> Dept. of Automation, Tsinghua University, Beijing 100084, China  
xpeng.cui@gmail.com, boyaoyang16@gmail.com, dcszj@tsinghua.edu.cn

## Abstract

Reinforcement Learning (RL) post-training has emerged as the dominant paradigm for eliciting mathematical reasoning in Large Language Models (LLMs), yet prevailing techniques such as GRPO and DAPO distribute rollout and gradient budgets nearly uniformly across prompts, squandering compute on samples that are already mastered or remain far beyond the model’s current capability. To address this fundamental inefficiency, we propose **Learning-Zone Energy** (LZE), a theoretically grounded, fully online data selection framework that concentrates computation on the model’s *active learning frontier*. At its core, we define a closed-form *Learning-Zone Energy Score* that fuses three complementary signals—an initial-difficulty anchor, a normalized outcome-uncertainty term, and a pass-rate momentum—into a single scalar that is provably aligned with the expected magnitude of group-relative policy gradient updates. A forward pruner with replay further reduces wall-clock time cost by skipping rollout generation for persistently solved prompts while periodically checking for forgetting. Evaluated on Qwen-family models (1.5B–8B) across GSM8K, MATH and DAPO-MATH, our method retains only 40% of the training data per step yet matches or surpasses full-data baselines, with especially pronounced out-of-distribution gains on AIME25(+45.9%) and AMC23(+18.2%), alongside an estimated 36% reduction in training FLOPs. Our code is available at <https://github.com/Stellaris167/LZE>.

## 1 Introduction

Reinforcement Learning (RL) with verifiable rewards has emerged as the dominant paradigm for improving mathematical reasoning in Large Language Models [5, 22]. In modern group-based RL pipelines such as GRPO [2, 27] and DAPO [44], the model generates multiple rollouts for each prompt, aggregates rewards within each group, and performs policy updates accordingly. However, these methods treat prompt groups nearly uniformly during training, even though the groups are highly heterogeneous in their usefulness: some prompts are already solved reliably and therefore contribute little additional learning signal, whereas others remain far beyond the model’s current capability and produce almost no actionable gradient information. Consequently, a considerable fraction of the rollout and optimization budget is spent on prompt groups that are only weakly informative for policy improvement.

To mitigate this inefficiency, prior work has explored curriculum-style training, offline filtering, and online rejection-based heuristics. Early work on curriculum learning and self-paced learning showed that training efficiency can benefit from organizing examples by difficulty [4, 14]. In the

---

\*Equal contribution.

<sup>†</sup>Corresponding author.

context of LLM post-training, offline filtering and self-training style methods can remove obviously uninformative examples before optimization begins [9, 30]. However, such strategies are inherently static and cannot adapt as the policy evolves and the effective difficulty of a prompt changes over time. Online rejection methods are more adaptive, yet they typically apply binary keep-or-drop decisions once a prompt becomes all-correct or all-incorrect [8, 39], making them insensitive to finer-grained differences in informativeness. A more recent online selection method [21] avoids redundant rollouts by predicting prompt solvability via a hidden Markov model, but requires maintaining a learned generative state model, inevitably incurring additional computational overhead. Therefore, existing approaches are often either static, overly rigid, or expensive. What is still missing is a lightweight online criterion that continuously adapts to the current policy, assigns prompt groups a graded notion of informativeness, and improves training efficiency without relying on heavy auxiliary machinery.

To address this gap, we propose **Learning-Zone Energy (LZE)**, a simple and fully online data selection framework for RL post-training. Our key idea is to prioritise prompt groups in the model’s current *learning zone*: groups that are neither already mastered nor completely out of reach, but actively capable of producing meaningful policy updates. Concretely, we define an *Energy Score* that combines three signals: an *initial-difficulty anchor* that preserves attention on historically challenging prompts, a *normalized uncertainty term* based on the current group pass rate that emphasises prompts near the decision boundary, and a *momentum term* that highlights groups on which the policy is actively changing. Beyond this practical intuition, we provide theoretical analysis for the design: in group-relative RL with Bernoulli rewards, the uncertainty term is aligned with the expected GRPO gradient variance under a standard fixed-baseline approximation (Theorem 1), thereby explaining why frontier prompt groups are especially informative. We further show that the momentum term corresponds to the output of a causal high-pass filter on the pass-rate sequence (Proposition 2), and that the score as a whole admits an interpretation as a sample-level attention mechanism. To further reduce training cost, we complement the backward scorer with a replay-based *forward pruner* that skips rollout generation for prompts that have remained solved over consecutive epochs, with periodic replay to detect forgetting.

Our contributions are threefold:

- **A principled online data selection framework.** The Learning-Zone Energy Score is a closed-form, per-step criterion that integrates difficulty history, outcome uncertainty, and pass-rate momentum into a single scalar provably aligned with the GRPO gradient variance. As it operates solely on group-level pass-rate statistics, LZE is compatible with any group-based RL post-training algorithm and requires no modification to the underlying optimizer. Retaining only 40% of prompts per training step, LZE matches and even surpasses full-data baselines across all evaluated configurations, with particularly pronounced out-of-distribution gains: up to +45.9% on AIME 25 and +18.2% on AMC 23.
- **Theoretical analysis of gradient informativeness in RL post-training.** We prove that the Bernoulli variance  $4p(1-p)$  governs the GRPO gradient variance up to a small-step-size approximation (Theorem 1), establish an EMA–convolution duality linking the momentum term to causal high-pass filtering of the pass-rate sequence (Proposition 2).
- **Compute efficiency via dual-stage selection.** The backward selector and forward pruner together reduce theoretical training FLOPs by an estimated 36%, consistent with the empirical FLOPs measurements across all model and dataset configurations reported in Table 1.

## 2 Background

We review the group-based RL post-training paradigm, introduce the notation used throughout, and identify the gradient-informativeness property that motivates our approach.

**RL post-training for mathematical reasoning.** Given a prompt dataset  $\mathcal{D} = \{x_i\}_{i=1}^N$  and a policy  $\pi_\theta$ , RL post-training maximises the expected reward:

$$\max_{\theta} \mathbb{E}_{x \sim \mathcal{D}, y \sim \pi_\theta(\cdot|x)} [r(x, y)], \quad (1)$$

where  $r(x, y) \in \{0, 1\}$  is a rule-based binary verifier that checks the correctness of response  $y$  for prompt  $x$ . This binary reward structure, standard in mathematical reasoning, makes the per-prompt *pass rate* a natural proxy for the policy’s current capability on that problem.

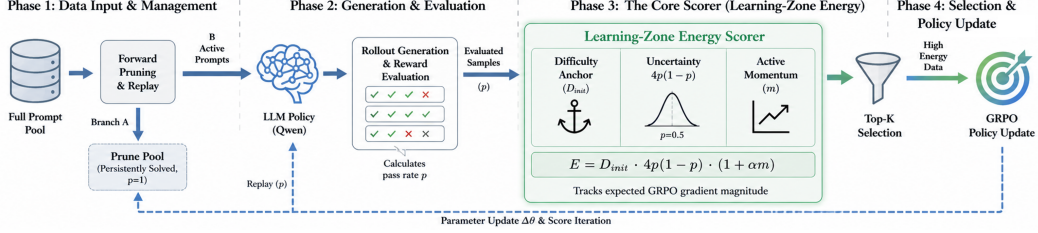


Figure 1: **Overview of the proposed method.** The backward scorer computes the Learning-Zone Energy Score for each prompt group at every training step, guiding Top- $K$  selection for policy updates. The forward pruner tracks group pass rates at the epoch level and skips rollout generation for groups that have been stably solved, with replay providing a safety mechanism to detect forgetting.

**Group Relative Policy Optimization (GRPO).** GRPO [2, 27] optimizes Eq. (1) without a learned value network by normalizing rewards within each sampled group. For prompt  $x_i$ , the policy generates  $n$  i.i.d. rollouts  $y_{i,1}, \dots, y_{i,n} \sim \pi_\theta(\cdot | x_i)$  with binary rewards  $r_{i,k} = r(x_i, y_{i,k})$ . The empirical pass rate  $p_i^{(t)} = n^{-1} \sum_k r_{i,k}$  serves as the group baseline, and the normalized group-relative advantage is

$$\tilde{A}_{i,k} = r_{i,k} - p_i^{(t)}. \quad (2)$$

GRPO then maximizes the clipped surrogate objective

$$\mathcal{L}_{\text{GRPO}}(\theta) = \frac{1}{N} \sum_{i=1}^N \frac{1}{n} \sum_{k=1}^n \min \left( \frac{\pi_\theta(y_{i,k} | x_i)}{\pi_{\theta_{\text{old}}}(y_{i,k} | x_i)} \tilde{A}_{i,k}, \text{clip} \left( \frac{\pi_\theta(y_{i,k} | x_i)}{\pi_{\theta_{\text{old}}}(y_{i,k} | x_i)}, 1-\epsilon, 1+\epsilon \right) \tilde{A}_{i,k} \right), \quad (3)$$

where the clipped importance ratio prevents  $\pi_\theta$  from deviating excessively from the behaviour policy  $\pi_{\theta_{\text{old}}}$  [26]. DAPO [44] removes the KL-divergence penalty from the reference policy and adopts a token-level entropy-aware clipping to further stabilize training, and all other aspects of the GRPO formulation are unchanged.

**Gradient informativeness and the learning zone.** Analyzing the gradient of Eq. (3) reveals a critical non-uniformity across prompt groups. Under the standard fixed-baseline approximation (treating  $p_i^{(t)}$  as constant when differentiating), the gradient contribution from prompt  $i$  is proportional to

$$\nabla_\theta \mathcal{L}^{(i)} \propto \frac{1}{n} \sum_{k=1}^n \tilde{A}_{i,k} \nabla_\theta \log \pi_\theta(y_{i,k} | x_i). \quad (4)$$

When  $p_i^{(t)} \rightarrow 1$ , all rollouts succeed and every advantage  $\tilde{A}_{i,k} \approx 0$ , so the gradient vanishes regardless of the policy’s score-function magnitude. Symmetrically, when  $p_i^{(t)} \rightarrow 0$ , all rollouts fail and advantages again collapse. As Theorem 1 formalizes, the variance of this gradient estimator is approximately proportional to the Bernoulli variance  $p_i(1 - p_i)$ , which peaks at  $p = 0.5$  and vanishes at both extremes. This identifies the *learning zone*, the intermediate pass-rate regime, as the locus of maximum gradient informativeness, and motivates concentrating the training budget accordingly.

**Online data selection.** At each training step  $t$ , the *online data selection problem* is to identify a subset  $\mathcal{S}_t \subseteq \mathcal{D}$  with  $|\mathcal{S}_t| = \lfloor \kappa N \rfloor$  ( $\kappa \in (0, 1)$ ) that maximizes expected policy improvement per unit of compute, using only information available at step  $t$ . A practical criterion must be (i) updated online without offline pre-processing, (ii) aligned with the gradient signal characterised by Eq. (4), and (iii) computationally cheap, requiring no auxiliary models beyond the standard rollout phase.

### 3 Methodology

This section presents the LZE framework in three parts. We first introduce the Learning-Zone Energy Score and explain the design rationale behind each of its three components (Section 3.1). We then provide theoretical support for the design by connecting the score to the GRPO gradient variance and classical signal-processing constructs (Section 3.2). Finally, we describe how the Energy Score drives backward Top- $K$  selection and how a complementary forward pruner with replay reduces rollout generation cost (Section 3.3).

### 3.1 The Learning-Zone Energy Score

The key challenge in online data selection for RL post-training is to construct a criterion that remains adaptive to the policy’s evolving capability while staying aligned with the underlying gradient signal. Motivated by the observation in Section 2 that the GRPO gradient variance for prompt  $i$  scales with  $p_i(1 - p_i)$ , we propose a score that captures three complementary aspects of prompt informativeness: intrinsic difficulty, current outcome uncertainty, and recent learning dynamics. Formally, for prompt  $i$  at training step  $t$ , we define the **Learning-Zone Energy Score** as

$$E_i^{(t)} = \underbrace{D_i^{(0)}}_{\text{difficulty anchor}} \cdot \underbrace{4p_i^{(t)}(1 - p_i^{(t)})}_{\text{outcome uncertainty}} \cdot \underbrace{(1 + \alpha m_i^{(t)})}_{\text{momentum}}, \quad (5)$$

where the three multiplicative factors correspond to the three signals above and each plays a distinct and non-redundant role.

**Outcome uncertainty:**  $4p_i^{(t)}(1 - p_i^{(t)})$ . The central term is the normalized Bernoulli variance of the current pass rate, which lies in  $[0, 1]$ , peaks at  $p = 0.5$ , and vanishes at both extremes. This term directly implements the learning-zone intuition: it concentrates selection on prompt groups where outcomes are mixed, i.e., neither consistently correct nor consistently incorrect, and suppresses both extremes. By Theorem 1, the GRPO gradient variance for prompt  $i$  is approximately proportional to  $p_i(1 - p_i) G_i(\theta)$ , confirming this term as the primary driver of gradient informativeness. Unlike Focal Loss [16], which uses  $(1 - p)^\gamma$  and penalises easy positives but not hard negatives,  $4p(1 - p)$  is *symmetric*: it simultaneously down-weights both extremes, providing a balanced treatment of the two failure modes.

**Difficulty anchor:**  $D_i^{(0)}$ . Not all prompts near  $p = 0.5$  are equally valuable. Two prompts may have the same current pass rate but very different histories: one that was initially easy and has since regressed conveys different information from one that was initially hard and is now being cracked for the first time. We record the pass rate at the start of training and set  $D_i^{(0)} = 1 - p_i^{(0)} \in [0, 1]$ , encoding the intrinsic hardness of each prompt as a fixed prior that is never updated. This anchor prevents the curriculum from collapsing toward problems that were initially easy but happen to sit transiently near  $p = 0.5$  due to policy noise.

**Pass-rate momentum:**  $m_i^{(t)}$ . Even with difficulty and uncertainty both captured, a prompt stagnating near  $p = 0.5$  for many steps contributes less than one where the policy is actively improving. We track learning dynamics via an exponential moving average  $\mu_i^{(t)} = \lambda\mu_i^{(t-1)} + (1 - \lambda)p_i^{(t)}$  with decay  $\lambda \in (0, 1)$ , and define the momentum  $m_i^{(t)} = p_i^{(t)} - \mu_i^{(t-1)}$ , which is positive when the policy is improving and near zero when learning stagnates. The factor  $(1 + \alpha m_i)$  amplifies the improvement in prompts and is neutral otherwise. As formalized in Section 3.2,  $m_i^{(t)}$  is the output of a causal high-pass filter on the pass-rate sequence, capturing rapid changes while attenuating slow trends.

To provide intuition for why LZE improves over uniform training, Figure 4 (Appendix A) illustrates three representative prompt types: a trivially solved prompt ( $p \approx 1$ ) and an unsolvable prompt ( $p \approx 0$ ), both filtered out due to near-zero Energy, and a frontier prompt ( $p \approx 0.5$ ) that receives the highest score and is selected for policy updates.

### 3.2 Theoretical Analysis

We now explain why the uncertainty term in the Energy Score is well motivated from the perspective of prompt-level gradient informativeness, and provide the signal-processing characterization of the momentum term. Throughout, let  $p_i$  denote the true pass rate under the current policy, and let  $G_i(\theta) := \mathbb{E}_{y \sim \pi_\theta(\cdot | x_i)} [\|\nabla_\theta \log \pi_\theta(y | x_i)\|^2]$  denote the expected squared score-function norm.

**Theorem 1** (Uncertainty term and gradient variance). *Consider prompt  $i$  with  $n$  i.i.d. rollouts and gradient estimator  $g_i = n^{-1} \sum_k A_k \nabla_\theta \log \pi_\theta(y_k | x_i)$ , where  $A_k = r_k - p_i$  under the standard fixed-baseline approximation [36]. Assume the score-function norm is approximately homogeneous across reward outcomes as in Eq. (6):*

$$\mathbb{E}[\|\nabla_\theta \log \pi_\theta(y | x_i)\|^2 | r = 1] \approx \mathbb{E}[\|\nabla_\theta \log \pi_\theta(y | x_i)\|^2 | r = 0] = G_i(\theta). \quad (6)$$

Then Eq. (7) holds:

$$\text{Var}(g_i) \approx \frac{p_i(1 - p_i)}{n} G_i(\theta), \quad (7)$$

where the approximation holds when  $\|\nabla_{\theta} p_i\|^2 \ll p_i(1-p_i)G_i(\theta)$ . The variance is maximized at  $p_i = 0.5$  and vanishes at both  $p_i = 0$  and  $p_i = 1$ . Consequently,  $E_i$  is monotonically related to  $\text{Var}(g_i)$ , modulated by the difficulty anchor and momentum.

*Proof.* Under the fixed-baseline assumption,  $\tilde{A}_k = r_k - p_i$  with  $p_i$  fixed. Since rollouts  $y_1, \dots, y_n$  are i.i.d., the per-sample gradient estimates  $\hat{g}_k = \tilde{A}_k \nabla_{\theta} \log \pi_{\theta}(y_k | x_i)$  are mutually independent. By the variance decomposition for i.i.d. summands,

$$\text{Var}(g_i) = \frac{1}{n} \text{Var}(\hat{g}_1) = \frac{1}{n} (\mathbb{E}[\|\hat{g}_1\|^2] - \|\mathbb{E}[\hat{g}_1]\|^2). \quad (8)$$

For the first term, using the homogeneity approximation in Eq. (6),

$$\mathbb{E}[\|\hat{g}_1\|^2] = \mathbb{E}[\tilde{A}_1^2 \|\nabla_{\theta} \log \pi_{\theta}(y_1 | x_i)\|^2] \approx \mathbb{E}[\tilde{A}_1^2] G_i(\theta) = p_i(1-p_i) G_i(\theta). \quad (9)$$

For the second term  $\mathbb{E}[\hat{g}_1] = \nabla_{\theta} p_i(\theta)$ , so  $\|\mathbb{E}[\hat{g}_1]\|^2 = \|\nabla_{\theta} p_i\|^2$ . Substituting Eq. (9) and the identity  $\|\mathbb{E}[\hat{g}_1]\|^2 = \|\nabla_{\theta} p_i\|^2$  into Eq. (8) gives Eq. (10):

$$\text{Var}(g_i) = \frac{p_i(1-p_i) G_i(\theta) - \|\nabla_{\theta} p_i(\theta)\|^2}{n} \approx \frac{p_i(1-p_i)}{n} G_i(\theta), \quad (10)$$

where the last step drops the subdominant term under the stated condition. Hence the Bernoulli variance  $p_i(1-p_i)$  governs the dominant component of the prompt-level gradient variance, and the normalization  $4p(1-p) \in [0, 1]$  is a monotone rescaling with maximum at  $p = 0.5$ .  $\square$

**Momentum as a temporal change signal.** The momentum  $m_i^{(t)} = p_i^{(t)} - \mu_i^{(t-1)}$  measures how much the current pass rate deviates from recent history. To see why large  $|m_i|$  signals high gradient magnitude, consider the first-order Taylor expansion of  $\ell_i(\theta) = p_i(\theta)$  around  $\theta_{t-1}$ ,

$$\Delta p_i^{(t)} := p_i^{(t)} - p_i^{(t-1)} \approx (\nabla_{\theta} \ell_i(\theta_{t-1}))^{\top} \Delta \theta, \quad (11)$$

where  $\Delta \theta = \theta_t - \theta_{t-1}$ . Eq. (11), combined with Exponential Moving Average (EMA) smoothing, implies  $|m_i^{(t)}| \lesssim \|\nabla_{\theta} p_i\| \|\Delta \theta\|$  by Cauchy–Schwarz, so the momentum factor amplifies prompts where the policy is changing rapidly.

**Proposition 2** (EMA–convolution duality). *With  $\mu_i^{(0)} = p_i^{(0)}$ , the EMA  $\mu_i^{(t)} = \lambda \mu_i^{(t-1)} + (1-\lambda)p_i^{(t)}$  equals the causal convolution  $(h * p_i)(t)$  with kernel  $h(\tau) = (1-\lambda)\lambda^{\tau} \mathbf{1}_{\tau \geq 0}$ . Consequently,  $m_i^{(t)} = p_i^{(t)} - \mu_i^{(t-1)}$  is the output of a causal high-pass filter applied to  $\{p_i^{(s)}\}_{s \leq t}$ .*

*Proof.* Unrolling the recurrence gives  $\mu_i^{(t)} = \sum_{\tau=0}^t (1-\lambda)\lambda^{\tau} p_i^{(t-\tau)} = (h * p_i)(t)$ . Since  $m_i^{(t)} = p_i^{(t)} - \mu_i^{(t-1)}$ , the momentum equals the original signal minus a one-step-delayed smoothed version of itself, which is the output of the complementary high-pass filter isolating rapid temporal changes.  $\square$

**Interpretation via attention.** The Energy Score can be read, by analogy, as a sample-level attention weight:  $D_i^{(0)}$  acts as a key encoding intrinsic hardness,  $\mu_i^{(t)}$  as a query representing current model state, and  $4p(1-p)(1+\alpha m)$  as the normalized score, with Top- $K$  implementing hard attention. Compared to Focal Loss [16] (asymmetric in  $p$ , static) and OHEM [29] (loss-based, memoryless),  $E_i$  is symmetric in  $p$ , temporally aware via EMA, and gradient-aligned by Theorem 1.

### 3.3 Prompt Selection and Training Algorithm

**Backward selection.** At each training step  $t$ , LZE first collects rollouts for all prompts in the active pool, computes pass rates and Energy Scores via Eq. (5), and then retains the top- $\kappa$  fraction for policy optimization. To balance exploitation with exploration, small Gumbel perturbations are added before ranking:  $\tilde{E}_i = E_i^{(t)} + g_i$ ,  $g_i \sim \text{Gumbel}(0, 1)$ . The top- $K = \lfloor \kappa |\mathcal{A}| \rfloor$  prompts by perturbed score form  $\mathcal{S}_t$ ; only these groups participate in policy gradient updates. Backward selection mainly reduces optimization cost, and rollouts are still collected over the full active pool to update Energy Scores.

**Forward pruning with replay.** At the epoch level, if prompt  $i$  achieves full correctness ( $p_i = 1$ ) for  $T_{\text{prune}} = 2$  consecutive epochs, it is moved to a prune pool  $\mathcal{P}$  and skipped in future rollout generation. At the start of each epoch, a fraction  $\rho$  of  $\mathcal{P}$  is re-evaluated, and any prompt that no longer achieves full correctness is restored to the active pool. The two stages are complementary: the backward selector concentrates the gradient budget on the most informative groups, while the forward pruner eliminates rollout cost for persistently solved prompts. The complete training procedure is presented in Algorithm 1.

---

**Algorithm 1** Learning-Zone Energy Training

---

**Require:** Dataset  $\mathcal{D}$ , policy  $\pi_{\theta_0}$ , selection ratio  $\kappa$ , EMA decay  $\lambda$ , momentum weight  $\alpha$ , prune threshold  $T_{\text{prune}}$ , replay ratio  $\rho$

- 1: **Initialise:** Run a single forward pass over  $\mathcal{D}$ ; for each  $i$ , compute  $p_i^{(0)}$ , set  $D_i^{(0)} \leftarrow 1 - p_i^{(0)}$ ,  $\mu_i^{(0)} \leftarrow p_i^{(0)}$ , epoch-correct counter  $c_i \leftarrow 0$
  - 2: Active pool  $\mathcal{A} \leftarrow \mathcal{D}$ ; Prune pool  $\mathcal{P} \leftarrow \emptyset$
  - 3: **for** each epoch  $e = 1, 2, \dots$  **do**
  - 4:     **Replay:** Sample  $\lfloor \rho |\mathcal{P}| \rfloor$  prompts from  $\mathcal{P}$ ; run rollouts; move any with  $p_i < 1$  back to  $\mathcal{A}$
  - 5:     **for** each training step  $t$  within epoch  $e$  **do**
  - 6:         Collect rollouts for all  $i \in \mathcal{A}$ ; compute  $p_i^{(t)}$
  - 7:          $\mu_i^{(t)} \leftarrow \lambda \mu_i^{(t-1)} + (1 - \lambda) p_i^{(t)}$  ▷ EMA update
  - 8:          $m_i^{(t)} \leftarrow p_i^{(t)} - \mu_i^{(t-1)}$  ▷ Momentum
  - 9:          $E_i^{(t)} \leftarrow D_i^{(0)} \cdot 4p_i^{(t)}(1 - p_i^{(t)}) \cdot (1 + \alpha m_i^{(t)})$  ▷ Energy Score
  - 10:          $\mathcal{S}_t \leftarrow \text{Gumbel-Top-K}(\{E_i^{(t)}\}_{i \in \mathcal{A}}, \lfloor \kappa |\mathcal{A}| \rfloor)$  ▷ Backward selection
  - 11:          $\theta_{t+1} \leftarrow \text{GradStep}(\pi_{\theta_t}, \mathcal{S}_t)$  ▷ Policy update on selected subset
  - 12:     **end for**
  - 13:     **Forward pruning:** For each  $i \in \mathcal{A}$ , increment  $c_i$  if  $p_i^{(t_{\text{last}})} = 1$ , else reset  $c_i \leftarrow 0$ ; if  $c_i \geq T_{\text{prune}}$ , move  $i$  from  $\mathcal{A}$  to  $\mathcal{P}$
  - 14: **end for**
- 

## 4 Experiments

We evaluate LZE on mathematical reasoning benchmarks across multiple model scales, comparing against representative data selection methods spanning offline filtering, online and SFT-based rejection. We further analyze training efficiency and convergence dynamics and conduct ablation studies to verify the contribution of each Energy Score component and the sensitivity to key hyperparameters.

**Models and Datasets.** We evaluate our method on mathematical reasoning, where models must produce step-by-step Chain-of-Thought (CoT) reasoning together with a boxed final answer. To ensure broad coverage, we experiment with models from the Qwen2.5 [40] and Qwen3 [42] families (the latter with thinking mode enabled throughout training), and the full list of evaluated variants is given in Table 1. Ablation studies are primarily conducted with Qwen2.5-Math-1.5B and -7B [41], chosen for their strong performance ceiling and stable inference behaviour, making them reliable starting points for post-training. We train on three datasets of increasing difficulty: GSM8K [7], MATH [11], and DAPO-MATH (English split) [44]. More details are provided in Appendix B.

**Hyper-parameters.** We follow the default configurations of the Verl framework [28] for PPO and GRPO training. Following recent practice in group-based RL post-training [10, 44], we remove the KL-divergence penalty and use temperature = 1.0, top- $p$  = 1.0, and top- $k$  = -1 to encourage diverse rollout generation. All runs use AdamW with learning rate  $1 \times 10^{-6}$ . The prompt batch size is 1024 for models under 4B parameters and 512 for larger models, with  $n = 8$  rollouts per prompt. Maximum generation length is 4096 tokens for Qwen2.5-family models and 16384 tokens for Qwen3-family models. The selection ratio  $k=0.4$  and momentum coefficient  $\alpha = 0.3$  are fixed across all main experiments, and sensitivity analyses are in Section 4.2.

**Evaluation.** We use a standardized chat template (Appendix C) and determine correctness via rule-based answer matching using `math-verify`. We report Pass@1 accuracy on both in-domain and out-of-distribution (OOD) benchmarks, together with estimated FLOPs budgets, wall-clock training time, and convergence speed.

### 4.1 Main Results

**Accuracy and out-of-distribution generalization.** Table 1 summarizes the Pass@1 accuracy across both in-domain and out-of-distribution (OOD) mathematical benchmarks. We report *Base* as the strong baseline without data filtering. Our method consistently outperforms the full-data baseline in nearly all configurations while training on only 40% of prompts per step, confirming that concentrating the gradient budget on the learning frontier is more effective than uniform allocation.

Table 1: Main Performance & Efficiency. Pass@1 comparison on in-domain and OOD evaluation sets, alongside estimated computational savings.

Training Set	Model		Accuracy (Pass@1)					FLOPs Budget	
			GSM8K	MATH	DAPO-MATH	AMC23	AIME25		Avg
GSM8K	Qwen2.5-Math-1.5B	Base	0.859	0.538	0.249	0.575	0.111	0.466	$5.47 \times 10^{19}$
		Ours	<b>0.860</b>	<b>0.553</b> <sup>†+2.8%</sup>	<b>0.265</b> <sup>†+6.4%</sup>	<b>0.600</b> <sup>†+4.3%</sup>	<b>0.122</b> <sup>†+9.9%</sup>	<b>0.480</b> <sup>†+2.9%</sup>	$3.50 \times 10^{19}$
	Qwen3-1.7B	Base	0.904	0.573	0.450	0.600	0.211	0.548	$4.94 \times 10^{19}$
		Ours	<b>0.912</b>	<b>0.578</b>	<b>0.452</b>	<b>0.700</b> <sup>†+16.7%</sup>	<b>0.267</b> <sup>†+26.5%</sup>	<b>0.582</b> <sup>†+6.2%</sup>	$3.17 \times 10^{19}$
MATH	Qwen2.5-Math-1.5B	Base	0.807	<b>0.583</b>	0.281	0.550	0.122	0.469	$5.82 \times 10^{19}$
		Ours	<b>0.825</b> <sup>†+2.2%</sup>	<b>0.583</b>	<b>0.310</b> <sup>†+10.3%</sup>	<b>0.650</b> <sup>†+18.2%</sup>	<b>0.178</b> <sup>†+45.9%</sup>	<b>0.509</b> <sup>†+8.6%</sup>	$3.73 \times 10^{19}$
	Qwen2.5-Math-7B	Base	0.868	0.621	0.440	0.700	0.278	0.581	$1.70 \times 10^{20}$
		Ours	0.876	<b>0.628</b>	<b>0.462</b> <sup>†+3.1%</sup>	<b>0.725</b> <sup>†+3.6%</sup>	<b>0.311</b> <sup>†+11.9%</sup>	<b>0.600</b> <sup>†+3.2%</sup>	$1.09 \times 10^{20}$
	Qwen3-4B	Base	<b>0.945</b>	0.771	0.576 <sup>‡</sup>	0.875	0.544	0.742	$1.18 \times 10^{20}$
		Ours	0.942	<b>0.775</b>	0.576 <sup>‡</sup>	<b>0.900</b> <sup>†+2.9%</sup>	<b>0.556</b> <sup>†+2.2%</sup>	<b>0.750</b> <sup>†+1.0%</sup>	$7.55 \times 10^{19}$
DAPO-MATH	Qwen2.5-Math-7B	Base	<b>0.928</b>	0.699	0.530	0.775	0.344	0.655	$2.94 \times 10^{20}$
		Ours	<b>0.928</b>	<b>0.708</b> <sup>†+1.3%</sup>	<b>0.546</b> <sup>†+3.0%</sup>	<b>0.825</b> <sup>†+6.5%</sup>	<b>0.356</b> <sup>†+3.5%</sup>	<b>0.673</b> <sup>†+2.7%</sup>	$1.89 \times 10^{20}$
	Qwen3-4B	Base	0.914	0.630	<b>0.807</b>	<b>0.925</b>	0.544	0.764	$8.56 \times 10^{19}$
		Ours	<b>0.941</b> <sup>†+3.0%</sup>	<b>0.639</b> <sup>†+1.4%</sup>	0.795	0.900	<b>0.556</b> <sup>†+2.2%</sup>	<b>0.766</b> <sup>†+0.3%</sup>	$5.48 \times 10^{19}$
	Qwen3-8B	Base	0.906	0.626	0.768	0.825	0.456	0.716	$9.85 \times 10^{19}$
		Ours	<b>0.911</b>	<b>0.630</b>	<b>0.807</b> <sup>†+5.1%</sup>	<b>0.925</b> <sup>†+12.1%</sup>	<b>0.500</b> <sup>†+9.6%</sup>	<b>0.755</b> <sup>†+5.4%</sup>	$6.30 \times 10^{19}$

The gains are most pronounced on the challenging OOD benchmarks AMC 23 and AIME 25, which measure transferable mathematical reasoning rather than in-distribution recall. Representative gains include: Qwen2.5-Math-1.5B on MATH achieving +45.9% on AIME 25 and +18.2% on AMC 23; Qwen3-1.7B on GSM8K achieving +26.5% on AIME 25 and +16.7% on AMC 23; and Qwen3-8B on DAPO-MATH achieving +12.1% on AMC 23 and +9.6% on AIME 25.

These OOD improvements are consistent with the theoretical prediction of Theorem 1: by suppressing both trivially solved and completely failed prompt groups, LZE prevents the policy from overfitting to the in-distribution difficulty profile, driving capability gains that transfer more broadly. The gains are particularly pronounced for smaller models (1.5B and 1.7B), where the learning zone is narrower and the Energy Score’s discriminative power is highest. Furthermore, consistent improvements across all scales from 1.5B to 8B and across both the Qwen2.5 and Qwen3 families confirm that learning-zone targeting is broadly applicable and not tied to any particular architecture or capacity regime.

**Efficiency and training progress.** The proposed data selection method reduces theoretical training FLOPs by approximately 36% by restricting backpropagation to the top-40% fraction of prompt groups, while maintaining full rollout coverage to recompute Energy Scores at each step (see Appendix E for the derivation). Figure 2 plots Pass@1 against wall-clock training time. For Qwen2.5-Math-1.5B, the baseline stabilizes at 3.97 hours; LZE reaches better performance in 2.40 hours (1.65× faster). For the 7B model, convergence is reached in 3.51 hours versus 4.92 hours for the baseline (1.40× faster). Adding the forward pruner yields further speedups of 1.80× and 1.91× for the 1.5B and 7B models, respectively, at a modest accuracy trade-off relative to the backward-only variant. Notably, uniform sampling at the same 40% retention ratio consistently underperforms the full-data baseline and even falls below the forward pruner in final accuracy, confirming that the gains of LZE stem from the principled identification of learning-zone prompts rather than from any implicit regularization effect of reduced data volume.

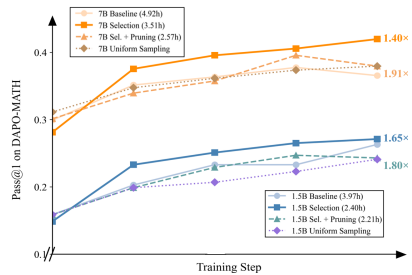


Figure 2: Pass@1 vs. wall-clock time for Qwen2.5-Math models. The × annotations denote speedup multipliers relative to the full-data baseline.

**Comparison with existing methods.** Table 2 compares LZE against offline, online, and SFT-based baselines on the MATH dataset, and empirical results suggest:

- *Offline filtering is ceiling-limited by an off-policy data distribution.* All Pre-Filter variants improve marginally over the baseline, but their gains plateau as training progresses. Static filters commit to

Table 2: Comparison of Pass@1 performance between the proposed method and existing data filtering baselines on the MATH dataset. All reported metrics represent the highest Pass@1 score achieved across the entire training trajectory. “rem.” stands for remove.

Method	Qwen2.5-Math-1.5B				Qwen2.5-Math-7B			
	DAPO-MATH	AMC23	AIME25	Avg Score	DAPO-MATH	AMC23	AIME25	Avg Score
Baseline	0.281	0.575	0.122	0.326	0.448	0.700	0.278	0.475
Ours	0.310	<b>0.650</b>	<b>0.178</b>	<b>0.379</b>	<b>0.462</b>	<b>0.725</b>	<b>0.311</b>	<b>0.500</b>
Reinforce-Rej (with online filtering)	0.235	0.525	0.122	0.294	0.351	<b>0.725</b>	0.200	0.425
Pre-Filter (rem. all wrong)	<b>0.327</b>	0.575	0.122	0.341	0.447	0.675	0.244	0.465
Pre-Filter (rem. all right)	0.305	0.575	0.167	0.349	0.458	0.675	0.279	0.471
Pre-Filter (discard all)	0.303	0.600	0.156	0.353	0.428	<b>0.725</b>	0.244	0.466
RAFT	0.281	0.575	0.133	0.330	0.363	0.575	0.189	0.348
Uniform sampling	0.273	0.550	0.122	0.315	0.437	0.675	0.289	0.467

a snapshot of model capability at initialization, but as the policy evolves, the curated distribution becomes increasingly off-policy and can no longer track the actual learning frontier. LZE recomputes its Energy Score at every training step, keeping the retained distribution continuously on-policy.

- *Binary online rejection destabilizes training.* Reinforce-Rej [39] permanently removes extreme-probability groups at first detection, disrupting the continuity of the training distribution and inducing optimization instability, as evidenced by its substantially lower OOD performance. LZE replaces hard removal with a continuous Energy Score for soft re-weighting, maintaining a stable training distribution without sacrificing adaptivity.
- *SFT-based filtering cannot substitute for RL exploration.* RAFT [8] retains only positively rewarded rollouts for supervised training and underperforms the full RL baseline on all benchmarks. This confirms that policy-gradient-driven exploration is essential for generalization: the diversity of the gradient signal cannot be recovered by SFT alone.

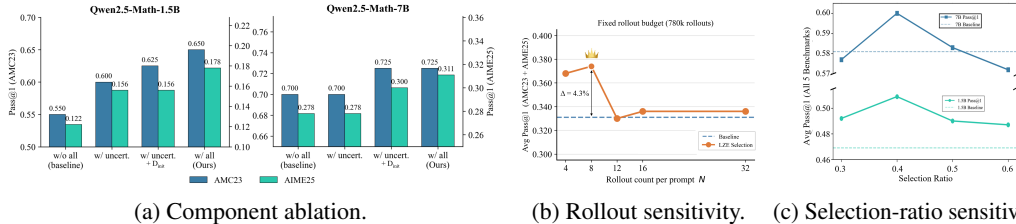


Figure 3: Ablation studies on Energy Score components, rollout count  $n$ , and selection ratio  $\kappa$ , conducted on Qwen2.5-Math models trained on MATH.

## 4.2 Ablation Study

**Contribution of each Energy Score component.** We ablate each factor in Eq. (5) by removing it in turn and measuring the resulting drop in Pass@1 on AMC23 and AIME25 using Qwen2.5-Math-1.5B and Qwen2.5-Math-7B. As shown in Figure 3a, removing the uncertainty term  $4p(1-p)$  causes the largest degradation, directly validating the learning-zone hypothesis of Theorem 1: gradient informativeness is maximized at  $p \approx 0.5$  and the uncertainty term is the primary driver of the improvement. Removing the difficulty anchor  $D_{\text{init}}$  allows the selector to collapse onto initially easy prompts that sit transiently near  $p = 0.5$  due to policy noise, reducing the quality of the retained set. Besides, removing the momentum term causes the selector to treat stagnating and actively improving prompts equivalently, weakening OOD generalization.

**Sensitivity to rollout  $n$ .** Under a fixed total rollout budget of 780k (corresponding to  $n=8$  over approximately 7 epochs), we vary the per-prompt rollout  $n \in \{4, 8, 12, 16, 32\}$  for both the baseline and LZE, holding all other hyperparameters constant. As shown in Figure 3b, LZE consistently outperforms the baseline across all values of  $n$ , with peak absolute performance at  $n=8$ . Smaller  $n$  reduces the number of samples used to estimate the group-level pass rate, making the Energy Score noisy and less discriminative. Larger  $n$  improves per-prompt accuracy but reduces the number of epochs within the fixed budget, limiting how many times the score can adapt to policy changes. The

default  $n=8$  strikes the best balance between estimate quality and adaptation frequency, and the performance gap between LZE and the baseline is most pronounced at this setting. Unconstrained upper-bound results are provided in Appendix F, which confirm that  $n=8$  remains a robust default across both efficiency-constrained and quality-maximizing regimes.

**Sensitivity to selection ratio  $k$ .** Figure 3c reports the averaged performance under varying  $\kappa$  across both the 1.5B and 7B models. and Pass@1 peaks at  $\kappa = 0.4$ . At lower ratios, the policy gradient becomes sample-starved and updates grow brittle. At higher ratios, prompts from the all-correct and all-incorrect regimes re-enter the training batch, diluting the gradient signal with uninformative updates, consistent with the prediction of Theorem 1 that  $\text{Var}(g_i)$  vanishes at both extremes.

## 5 Related Work

**Reinforcement Learning for Mathematical Reasoning.** Building on chain-of-thought reasoning [35], self-consistency decoding [34], and tree search [43, 47], reinforcement learning has become the dominant post-training paradigm for LLM reasoning. PPO [26] served as the canonical optimizer in early RLHF work [23], but REINFORCE-style variants have since gained traction for lower complexity and favourable scaling [3, 12, 36]. GRPO [2, 27] normalizes rewards within each prompt group to estimate advantages without a critic, and DAPO [44] improves stability through dynamic sampling and entropy-preserving clipping. Recent analysis suggests that the reasoning capacity of RL with verifiable rewards remains bounded by the base model’s distribution [19], and that data selection can matter as much as the optimizer [21, 39].

**Curriculum Learning and Data Selection.** Curriculum learning [4] and self-paced learning [14] established that organizing examples by difficulty improves optimization. In LLM post-training, data selection strategies prioritizing instances by quality, difficulty, or diversity have been shown to outperform naive quantity scaling [18, 31]. Difficulty-aware approaches use proxies such as instruction complexity [20], model uncertainty [13], focal weighting [16], and online hard-example mining [29] to concentrate the gradient budget on informative samples. Diversity-oriented methods complement these via semantic deduplication, quality-driven subset selection, and gradient-based influence estimation [1, 6, 37, 38, 49]. Token-level selection further refines this by allocating training signal only to informative tokens within each sequence [17]. Most of these approaches operate offline and cannot adapt to the evolving policy landscape of online RL.

**Data Filtering in RL Post-Training.** A growing body of work investigates data filtering during RL post-training, motivated by the observation that not all rollouts contribute equally to policy improvement. Offline pre-filtering removes prompts that are too easy or too hard via a one-time difficulty scoring pass [9, 30], but cannot adapt as the policy evolves. Online rejection methods, including Best-of- $N$  sampling [7, 45, 46], iterative self-training [8, 24], and Reinforce-Rej [39], operate adaptively but apply binary keep-or-drop decisions that discard the continuous gradient signal. Reward- and signal-driven re-weighting methods use curiosity signals or mistake patterns [25, 33]; process-level verification provides finer-grained filtering [15, 32], while generative reward modeling offers an alternative verifier design [48], all at the cost of auxiliary models. DPS [21], a recent method, reduces redundant rollouts by predicting prompt solvability via a hidden Markov model, but necessitates online Bayesian inference and a learned generative state model, inevitably incurring additional overhead. LZE differs from all of the above: the Energy Score is a continuous, closed-form criterion requiring no auxiliary models, and naturally subsumes binary filtering as a special case.

## 6 Conclusion

In this work, we propose **Learning-Zone Energy (LZE)**, a fully online data selection framework for efficient RL post-training. The central insight is that GRPO gradient variance is approximately proportional to the pass-rate variance  $p(1 - p)$ , which peaks in the intermediate regime where the model neither consistently succeeds nor consistently fails. Building on this, the Learning-Zone Energy Score fuses *initial difficulty*, *outcome uncertainty*, and *pass-rate momentum* into a closed-form criterion updated at every training step without auxiliary models. Empirical results demonstrate that LZE achieves superior performance on nearly all benchmarks while training on only 40% of prompts per step, with particularly pronounced gains on OOD settings. One limitation of the current study is that all experiments focus on mathematical reasoning tasks with binary verifiable rewards, so whether the same scoring rule transfers to open-ended or noisy-reward settings remains an important direction for future work.

## References

- [1] Amro Abbas, Kushal Tirumala, Daniel Simig, Surya Ganguli, and Ari S. Morcos. Semd-edup: Data-efficient learning at web-scale through semantic deduplication. *arXiv preprint arXiv:2303.09540*, 2023.
- [2] Deepseek AI. Deepseek-r1 incentivizes reasoning in llms through reinforcement learning. *Nature*, 645(8081):633–638, September 2025. ISSN 1476-4687. doi: 10.1038/s41586-025-09422-z.
- [3] Ahmadian Arash, Cremer Chris, Gallé Matthias, Fadaee Marzieh, Kreutzer Julia, Pietquin Olivier, Üstün Ahmet, and Hooker Sara. Back to basics: Revisiting REINFORCE-style optimization for learning from human feedback in LLMs. In *Proceedings of the 62nd Annual Meeting of the Association for Computational Linguistics (Volume 1: Long Papers)*, pages 12248–12267. Association for Computational Linguistics, August 2024. doi: 10.18653/v1/2024.acl-long.662.
- [4] Yoshua Bengio, Jérôme Louradour, Ronan Collobert, and Jason Weston. Curriculum learning. In *Proceedings of the 26th Annual International Conference on Machine Learning, ICML '09*, pages 41–48, 2009. ISBN 9781605585161. doi: 10.1145/1553374.1553380.
- [5] Tom Brown, Benjamin Mann, Nick Ryder, Melanie Subbiah, Jared D Kaplan, Prafulla Dhariwal, Arvind Neelakantan, Pranav Shyam, Girish Sastry, Amanda Askell, Sandhini Agarwal, Ariel Herbert-Voss, Gretchen Krueger, Tom Henighan, Rewon Child, Aditya Ramesh, Daniel Ziegler, Jeffrey Wu, Clemens Winter, Chris Hesse, Mark Chen, Eric Sigler, Mateusz Litwin, Scott Gray, Benjamin Chess, Jack Clark, Christopher Berner, Sam McCandlish, Alec Radford, Ilya Sutskever, and Dario Amodei. Language models are few-shot learners. In *Advances in Neural Information Processing Systems*, volume 33, pages 1877–1901, 2020.
- [6] Lichang Chen, Shiyang Li, Jun Yan, Hai Wang, Kalpa Gunaratna, Vikas Yadav, Zheng Tang, Vijay Srinivasan, Tianyi Zhou, Heng Huang, and Hongxia Jin. Alpargus: Training a better alpaca with fewer data. In *International Conference on Learning Representations (ICLR)*, pages 34767–34797, 2024.
- [7] Karl Cobbe, Vineet Kosaraju, Mohammad Bavarian, Mark Chen, Heewoo Jun, Lukasz Kaiser, Matthias Plappert, Jerry Tworek, Jacob Hilton, Reiichiro Nakano, Christopher Hesse, and John Schulman. Training verifiers to solve math word problems, 2021.
- [8] Hanze Dong, Wei Xiong, Deepanshu Goyal, Yihan Zhang, Winnie Chow, Rui Pan, Shizhe Diao, Jipeng Zhang, KaShun SHUM, and Tong Zhang. RAFT: Reward ranked finetuning for generative foundation model alignment. *Transactions on Machine Learning Research*, 2023. ISSN 2835-8856.
- [9] Caglar Gulcehre, Tom Le Paine, Srivatsan Srinivasan, Ksenia Konyushkova, Lotte Weerts, Abhishek Sharma, Aditya Siddhant, Alex Ahern, Miaosen Wang, Chenjie Gu, Wolfgang Macherey, Arnaud Doucet, Orhan Firat, and Nando de Freitas. Reinforced self-training (rest) for language modeling, 2023.
- [10] Bingxiang He, Zekai Qu, Zeyuan Liu, Yinghao Chen, Yuxin Zuo, Cheng Qian, Kaiyan Zhang, Weize Chen, Chaojun Xiao, Ganqu Cui, Ning Ding, and Zhiyuan Liu. JustRL: Scaling a 1.5b LLM with a simple RL recipe, 2025.
- [11] Dan Hendrycks, Collin Burns, Saurav Kadavath, Akul Arora, Steven Basart, Eric Tang, Dawn Song, and Jacob Steinhardt. Measuring mathematical problem solving with the MATH dataset. In *Proceedings of the Neural Information Processing Systems Track on Datasets and Benchmarks*, volume 1, 2021.
- [12] Wouter Kool, Herke van Hoof, and Max Welling. Buy 4 REINFORCE samples, get a baseline for free! In *Deep Reinforcement Learning Meets Structured Prediction, ICLR 2019 Workshop, New Orleans, Louisiana, United States, May 6, 2019*, 2019.

- [13] Lorenz Kuhn, Yarin Gal, and Sebastian Farquhar. Semantic uncertainty: Linguistic invariances for uncertainty estimation in natural language generation. In *International Conference on Learning Representations (ICLR)*, 2023.
- [14] M. Kumar, Benjamin Packer, and Daphne Koller. Self-paced learning for latent variable models. In *Advances in Neural Information Processing Systems*, volume 23, pages 1189–1197, 2010.
- [15] Hunter Lightman, Vineet Kosaraju, Yuri Burda, Harrison Edwards, Bowen Baker, Teddy Lee, Jan Leike, John Schulman, Ilya Sutskever, and Karl Cobbe. Let’s verify step by step. In *International Conference on Learning Representations (ICLR)*, pages 39578–39601, 2024.
- [16] Tsung-Yi Lin, Priya Goyal, Ross Girshick, Kaiming He, and Piotr Dollar. Focal loss for dense object detection. In *2017 IEEE International Conference on Computer Vision (ICCV)*, pages 2999–3007, 2017. doi: 10.1109/ICCV.2017.324.
- [17] Zhenghao Lin, Zhibin Gou, Yeyun Gong, Xiao Liu, Yelong Shen, Ruochen Xu, Chen Lin, Yujiu Yang, Jian Jiao, Nan Duan, and Weizhu Chen. Not all tokens are what you need for pretraining. In *Advances in Neural Information Processing Systems*, volume 37, pages 29029–29063, 2024. doi: 10.52202/079017-0914.
- [18] Wei Liu, Weihao Zeng, Keqing He, Yong Jiang, and Junxian He. What makes good data for alignment? a comprehensive study of automatic data selection in instruction tuning. In *International Conference on Learning Representations (ICLR)*, pages 22353–22373, 2024.
- [19] Zichen Liu, Changyu Chen, Wenjun Li, Penghui Qi, Tianyu Pang, Chao Du, Wee Sun Lee, and Min Lin. Understanding rl-zero-like training: A critical perspective, 2025.
- [20] Keming Lu, Hongyi Yuan, Zheng Yuan, Runji Lin, Junyang Lin, Chuanqi Tan, Chang Zhou, and Jingren Zhou. #instag: Instruction tagging for analyzing supervised fine-tuning of large language models. In *International Conference on Learning Representations (ICLR)*, pages 36456–36474, 2024.
- [21] Yixiu Mao, Yun Qu, Cheems Wang, Heming Zou, and Xiangyang Ji. Dynamics-Predictive Sampling for Active RL Finetuning of Large Reasoning Models. In *International Conference on Learning Representations (ICLR)*, 2026.
- [22] OpenAI. Gpt-4 technical report, 2023.
- [23] Long Ouyang, Jeffrey Wu, Xu Jiang, Diogo Almeida, Carroll Wainwright, Pamela Mishkin, Chong Zhang, Sandhini Agarwal, Katarina Slama, Alex Ray, John Schulman, Jacob Hilton, Fraser Kelton, Luke Miller, Maddie Simens, Amanda Askell, Peter Welinder, Paul F Christiano, Jan Leike, and Ryan Lowe. Training language models to follow instructions with human feedback. In S. Koyejo, S. Mohamed, A. Agarwal, D. Belgrave, K. Cho, and A. Oh, editors, *Advances in Neural Information Processing Systems*, volume 35, pages 27730–27744. Curran Associates, Inc., 2022.
- [24] Richard Yuanzhe Pang, Weizhe Yuan, Kyunghyun Cho, He He, Sainbayar Sukhbaatar, and Jason Weston. Iterative Reasoning Preference Optimization. In A. Globerson, L. Mackey, D. Belgrave, A. Fan, U. Paquet, J. Tomczak, and C. Zhang, editors, *Advances in Neural Information Processing Systems*, volume 37, pages 116617–116637. Curran Associates, Inc., 2024. doi: 10.52202/079017-3702.
- [25] Deepak Pathak, Pulkit Agrawal, Alexei A. Efros, and Trevor Darrell. Curiosity-driven exploration by self-supervised prediction. In *2017 IEEE Conference on Computer Vision and Pattern Recognition Workshops (CVPRW)*, pages 488–489, 2017. doi: 10.1109/CVPRW.2017.70.
- [26] John Schulman, Filip Wolski, Prafulla Dhariwal, Alec Radford, and Oleg Klimov. Proximal policy optimization algorithms, 2017.
- [27] Zhihong Shao, Peiyi Wang, Qihao Zhu, Runxin Xu, Junxiao Song, Xiao Bi, Haowei Zhang, Mingchuan Zhang, Y. K. Li, Y. Wu, and Daya Guo. Deepseekmath: Pushing the limits of mathematical reasoning in open language models, 2024.

- [28] Guangming Sheng, Chi Zhang, Zilingfeng Ye, Xibin Wu, Wang Zhang, Ru Zhang, Yanghua Peng, Haibin Lin, and Chuan Wu. Hybridflow: A flexible and efficient rlhf framework. In *Proceedings of the Twentieth European Conference on Computer Systems*, pages 1279–1297. ACM, March 2025. doi: 10.1145/3689031.3696075. URL <http://dx.doi.org/10.1145/3689031.3696075>.
- [29] Abhinav Shrivastava, Abhinav Gupta, and Ross Girshick. Training region-based object detectors with online hard example mining. In *Proceedings of the IEEE Conference on Computer Vision and Pattern Recognition*, pages 761–769, June 2016.
- [30] Avi Singh, John D Co-Reyes, Rishabh Agarwal, Ankesh Anand, Piyush Patil, Xavier Garcia, Peter J Liu, James Harrison, Jaehoon Lee, Kelvin Xu, Aaron T Parisi, Abhishek Kumar, Alexander A Alemi, Alex Rizkowsky, Azade Nova, Ben Adlam, Bernd Bohnet, Gamaleldin Fathy Elsayed, Hanie Sedghi, Igor Mordatch, Isabelle Simpson, Izzeddin Gur, Jasper Snoek, Jeffrey Pennington, Jiri Hron, Kathleen Kenealy, Kevin Swersky, Kshiteej Mahajan, Laura A Culp, Lechao Xiao, Maxwell Bileschi, Noah Constant, Roman Novak, Rosanne Liu, Tris Warkentin, Yamini Bansal, Ethan Dyer, Behnam Neyshabur, Jascha Sohl-Dickstein, and Noah Fiedel. Beyond human data: Scaling self-training for problem-solving with language models. *Transactions on Machine Learning Research*, 2024. ISSN 2835-8856.
- [31] Ben Sorscher, Robert Geirhos, Shashank Shekhar, Surya Ganguli, and Ari Morcos. Beyond neural scaling laws: beating power law scaling via data pruning. In *Advances in Neural Information Processing Systems*, volume 35, pages 19523–19536, 2022.
- [32] Jonathan Uesato, Nate Kushman, Ramana Kumar, Francis Song, Noah Siegel, Lisa Wang, Antonia Creswell, Geoffrey Irving, and Irina Higgins. Solving math word problems with process- and outcome-based feedback, 2022.
- [33] Danqing Wang and Lei Li. Learning from mistakes via cooperative study assistant for large language models. In *Proceedings of the 2023 Conference on Empirical Methods in Natural Language Processing*, pages 10667–10685, December 2023. doi: 10.18653/v1/2023.emnlp-main.659.
- [34] Xuezhi Wang, Jason Wei, Dale Schuurmans, Quoc V Le, Ed H. Chi, Sharan Narang, Aakanksha Chowdhery, and Denny Zhou. Self-consistency improves chain of thought reasoning in language models. In *International Conference on Learning Representations (ICLR)*, 2023.
- [35] Jason Wei, Xuezhi Wang, Dale Schuurmans, Maarten Bosma, Brian Ichter, Fei Xia, Ed Chi, Quoc V Le, and Denny Zhou. Chain-of-thought prompting elicits reasoning in large language models. In *Advances in Neural Information Processing Systems*, volume 35, pages 24824–24837, 2022.
- [36] Ronald J. Williams. Simple statistical gradient-following algorithms for connectionist reinforcement learning. *Mach. Learn.*, 8(3-4):229–256, May 1992. ISSN 0885-6125. doi: 10.1007/BF00992696.
- [37] Mengzhou Xia, Sadhika Malladi, Suchin Gururangan, Sanjeev Arora, and Danqi Chen. LESS: Selecting influential data for targeted instruction tuning. In *Forty-first International Conference on Machine Learning*, Proceedings of Machine Learning Research, pages 54104–54132, 2024.
- [38] Sang Michael Xie, Shibani Santurkar, Tengyu Ma, and Percy S Liang. Data selection for language models via importance resampling. In *Advances in Neural Information Processing Systems*, volume 36, pages 34201–34227, 2023.
- [39] Wei Xiong, Jiarui Yao, Yuhui Xu, Bo Pang, Lei Wang, Doyen Sahoo, Junnan Li, Nan Jiang, Tong Zhang, Caiming Xiong, and Hanze Dong. A minimalist approach to LLM reasoning: from rejection sampling to reinforce, 2025.
- [40] An Yang, Baosong Yang, Beichen Zhang, Binyuan Hui, Bo Zheng, Bowen Yu, Chengyuan Li, Dayiheng Liu, Fei Huang, Haoran Wei, Huan Lin, Jian Yang, Jianhong Tu, Jianwei Zhang, Jianxin Yang, Jiayi Yang, Jingren Zhou, Junyang Lin, Kai Dang, Keming Lu, Keqin Bao, Kexin Yang, Le Yu, Mei Li, Mingfeng Xue, Pei Zhang, Qin Zhu, Rui Men, Runji Lin, Tianhao Li, Tianyi Tang, Tingyu Xia, Xingzhang Ren, Xuancheng Ren, Yang Fan, Yang Su, Yichang Zhang,

- Yu Wan, Yuqiong Liu, Zeyu Cui, Zhenru Zhang, and Zihan Qiu. Qwen2.5 technical report, 2024.
- [41] An Yang, Beichen Zhang, Binyuan Hui, Bofei Gao, Bowen Yu, Chengpeng Li, Dayiheng Liu, Jianhong Tu, Jingren Zhou, Junyang Lin, Keming Lu, Mingfeng Xue, Runji Lin, Tianyu Liu, Xingzhang Ren, and Zhenru Zhang. Qwen2.5-math technical report: Toward mathematical expert model via self-improvement, 2024.
- [42] An Yang, Anfeng Li, Baosong Yang, Beichen Zhang, Binyuan Hui, Bo Zheng, Bowen Yu, Chang Gao, Chengen Huang, Chenxu Lv, Chujie Zheng, Dayiheng Liu, Fan Zhou, Fei Huang, Feng Hu, Hao Ge, Haoran Wei, Huan Lin, Jialong Tang, Jian Yang, Jianhong Tu, Jianwei Zhang, Jianxin Yang, Jiayi Yang, Jing Zhou, Jingren Zhou, Junyang Lin, Kai Dang, Keqin Bao, Kexin Yang, Le Yu, Lianghao Deng, Mei Li, Mingfeng Xue, Mingze Li, Pei Zhang, Peng Wang, Qin Zhu, Rui Men, Ruize Gao, Shixuan Liu, Shuang Luo, Tianhao Li, Tianyi Tang, Wenbiao Yin, Xingzhang Ren, Xinyu Wang, Xinyu Zhang, Xuancheng Ren, Yang Fan, Yang Su, Yichang Zhang, Yinger Zhang, Yu Wan, Yuqiong Liu, Zekun Wang, Zeyu Cui, Zhenru Zhang, Zhipeng Zhou, and Zihan Qiu. Qwen3 technical report, 2025.
- [43] Shunyu Yao, Dian Yu, Jeffrey Zhao, Izhak Shafran, Tom Griffiths, Yuan Cao, and Karthik Narasimhan. Tree of thoughts: Deliberate problem solving with large language models. In A. Oh, T. Naumann, A. Globerson, K. Saenko, M. Hardt, and S. Levine, editors, *Advances in Neural Information Processing Systems*, volume 36, pages 11809–11822. Curran Associates, Inc., 2023.
- [44] Qiyang Yu, Zheng Zhang, Ruofei Zhu, Yufeng Yuan, Xiaochen Zuo, Yu Yue, Weinan Dai, Tiantian Fan, Gaohong Liu, juncai liu, LingJun Liu, Xin Liu, Haibin Lin, Zhiqi Lin, Bole Ma, Guangming Sheng, Yuxuan Tong, Chi Zhang, Mofan Zhang, Ru Zhang, Wang Zhang, Hang Zhu, Jinhua Zhu, Jiaye Chen, Jiangjie Chen, Chengyi Wang, Hongli Yu, Yuxuan Song, Xiangpeng Wei, Hao Zhou, Jingjing Liu, Wei-Ying Ma, Ya-Qin Zhang, Lin Yan, Yonghui Wu, and Mingxuan Wang. Dapo: An open-source llm reinforcement learning system at scale. In *Advances in Neural Information Processing Systems*, volume 38, pages 113222–113244, 2025.
- [45] Weizhe Yuan, Richard Yuanzhe Pang, Kyunghyun Cho, Xian Li, Sainbayar Sukhbaatar, Jing Xu, and Jason Weston. Self-rewarding language models, 2024.
- [46] Zheng Yuan, Hongyi Yuan, Chengpeng Li, Guanting Dong, Keming Lu, Chuanqi Tan, Chang Zhou, and Jingren Zhou. Scaling relationship on learning mathematical reasoning with large language models, 2023.
- [47] Eric Zelikman, Yuhuai Wu, Jesse Mu, and Noah Goodman. Star: Bootstrapping reasoning with reasoning. In S. Koyejo, S. Mohamed, A. Agarwal, D. Belgrave, K. Cho, and A. Oh, editors, *Advances in Neural Information Processing Systems*, volume 35, pages 15476–15488. Curran Associates, Inc., 2022.
- [48] Lunjun Zhang, Arian Hosseini, Hritik Bansal, Seyed Mehran Kazemi, Aviral Kumar, and Rishabh Agarwal. Generative verifiers: Reward modeling as next-token prediction. In *International Conference on Learning Representations (ICLR)*, pages 12476–12505, 2025.
- [49] Chunting Zhou, Pengfei Liu, Puxin Xu, Srinivasan Iyer, Jiao Sun, Yuning Mao, Xuezhe Ma, Avia Efrat, Ping Yu, LILI YU, Susan Zhang, Gargi Ghosh, Mike Lewis, Luke Zettlemoyer, and Omer Levy. Lima: Less is more for alignment. In *Advances in Neural Information Processing Systems*, volume 36, pages 55006–55021, 2023.

## **Appendices**

<b>A Case Study: Data Selection Rationale</b>	<b>15</b>
<b>B Details of Models and Datasets</b>	<b>15</b>
<b>C Chat Templates and Prompt Formatting</b>	<b>16</b>
<b>D Hardware and Runtime Details</b>	<b>16</b>
<b>E Detailed Computational Efficiency Analysis</b>	<b>16</b>
<b>F Additional Ablation Studies</b>	<b>17</b>
<b>G Use of LLMs</b>	<b>18</b>
<b>H Broader Impacts</b>	<b>18</b>

## A Case Study: Data Selection Rationale

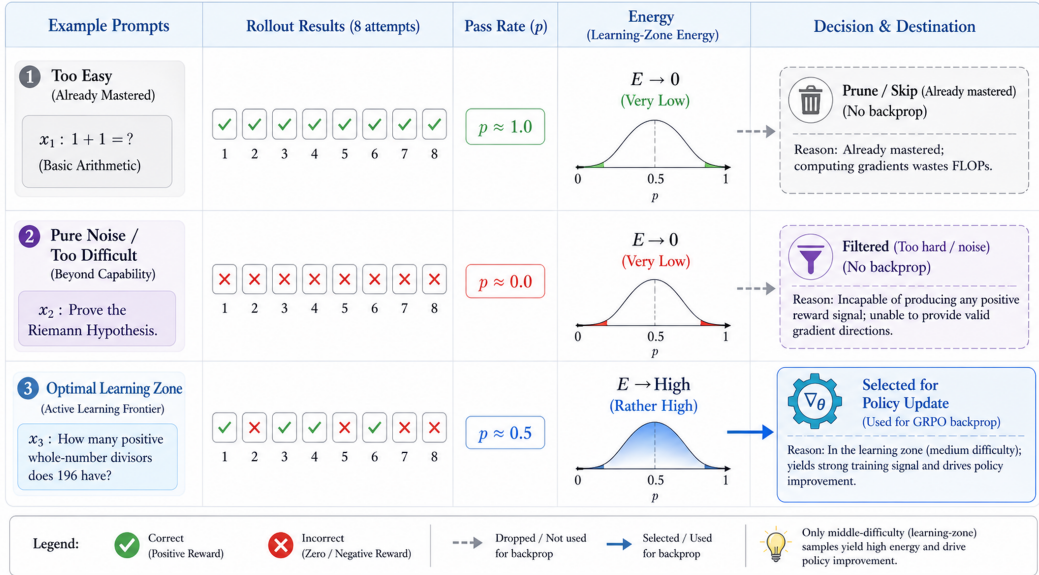


Figure 4: **Conceptual case study of the learning zone.** Trivial prompts that are already solved ( $p \approx 1$ ) and overwhelmingly hard prompts that consistently fail ( $p \approx 0$ ) carry negligible Learning-Zone Energy and are therefore deprioritized. In contrast, frontier prompts with mixed rollout outcomes ( $p \approx 0.5$ ) receive the highest uncertainty weight and remain actively selected for GRPO updates.

## B Details of Models and Datasets

**Models.** We evaluate two families of open-weight Qwen reasoning models. The Qwen2.5-Math line, including Qwen2.5-Math-1.5B-Instruct (<https://huggingface.co/Qwen/Qwen2.5-Math-1.5B-Instruct>) and Qwen2.5-Math-7B-Instruct (<https://huggingface.co/Qwen/Qwen2.5-Math-7B-Instruct>), is specialized for mathematical reasoning and provides our main math-centric backbone. The Qwen3 line, including Qwen3-1.7B (<https://huggingface.co/Qwen/Qwen3-1.7B>), Qwen3-4B (<https://huggingface.co/Qwen/Qwen3-4B>), and Qwen3-8B (<https://huggingface.co/Qwen/Qwen3-8B>), offers broader reasoning capacity and stronger general-purpose post-training behavior; for all Qwen3 experiments we enable thinking mode throughout training and evaluation. According to the corresponding Hugging Face model cards, all five checkpoints are released under the Apache-2.0 license.

**Datasets.** We train on three public mathematical reasoning datasets with progressively increasing difficulty. GSM8K (<https://huggingface.co/datasets/openai/gsm8k>) contains relatively short grade-school arithmetic word problems and serves as the easiest setting in our study. MATH ([https://huggingface.co/datasets/ElletherAI/hendrycks\\_math](https://huggingface.co/datasets/ElletherAI/hendrycks_math)) contains substantially harder competition-style problems spanning algebra, geometry, counting, and number theory. DAPO-MATH (English split; <https://huggingface.co/datasets/BytedTsinghua-SIA/DAPOMath-17k>) is the most challenging training source used here, with longer solution trajectories and more diverse reasoning patterns, making it especially suitable for probing efficiency gains under harder post-training regimes. For evaluation, we use the corresponding held-out test splits of GSM8K, MATH, and DAPO-MATH from the same repositories, together with the OOD benchmarks AMC23 (<https://huggingface.co/datasets/JingzeShi/amc23>) and AIME25 (<https://huggingface.co/datasets/math-ai/aime25>); these are exactly the benchmark sets reported in Table 1 and Table 2 of Section 4.

**Licenses.** The external assets used in our experiments are all taken from public model or dataset cards that state their licenses explicitly. The Qwen checkpoints are Apache-2.0; GSM8K and MATH

are MIT; DAPO-MATH and AIME25 are Apache-2.0; and the AMC23 mirror used in our evaluation setup is MIT.

## C Chat Templates and Prompt Formatting

### ChatML System and User Template

```
<|im_start|>system
You are a helpful mathematical reasoning assistant.
<|im_end|>
<|im_start|>user
Please reason step by step, and
put your final answer within \boxed{ }.
{Question}
<|im_end|>
<|im_start|>assistant
```

## D Hardware and Runtime Details

All experiments are conducted on 8 NVIDIA Blackwell-series GPUs. For runs trained on GSM8K or MATH, each configuration requires roughly 3.5 hours on average. Runs trained on DAPO-MATH are longer because of the more difficult prompts and longer reasoning trajectories, with an average duration of about 8 hours per configuration. Relative to the full-data baseline, our method reduces end-to-end runtime by approximately 30%–40% across the reported settings.

## E Detailed Computational Efficiency Analysis

In this section, we provide a rigorous mathematical derivation of the computational footprint associated with our reinforcement learning (RL) training pipeline. We contextualize our footprint within the standard veRL framework execution to derive the baseline theoretical coefficient of 10, which we partition into inference and optimization phases, measured in floating-point operations (FLOPs) per parameter per token.

Let  $P$  denote the number of parameters in the policy model, and  $T$  represent the average total sequence length ( $T = L_{\text{prompt}} + L_{\text{response}}$ ).

**Inference and Generation Cost.** During the data collection phase, the policy model autoregressively generates  $n_{\text{rollout}}$  responses for each prompt. Generating a single token requires a forward pass through the active policy network. In dense causal Transformer architectures, KV-cache-assisted token decoding incurs approximately  $2P$  FLOPs per token. Following standard engineering implementations of GRPO (e.g., the veRL framework using vLLM), the evaluation for the reference model logic is computationally merged or evaluated without gradient tracking. A reward model is subsequently invoked to evaluate the sequences, costing an additional  $2P$  FLOPs per token for the forward pass. Therefore, the generative inference scaling factor analytically resolves to: Eq. (12):

$$C_{\text{infer}} = \underbrace{2}_{\text{Actor Generation}} + \underbrace{2}_{\text{Reward Model Scoring}} = 4. \quad (12)$$

**Optimization and Update Cost.** During the optimization phase, only the actor (policy) model’s weights undergo iterative updates via backpropagation. No critic model is utilized in GRPO. For a decoder-only LLM, the optimization phase incorporates a forward pass (activations) and a backward pass (gradients with respect to activations and learnable weights). The forward pass necessitates  $2P$  FLOPs per token. The backward pass demands approximately  $4P$  FLOPs per token ( $2P$  for activation gradients, and  $2P$  for weight gradients). The underlying computational coefficient for optimization is modeled strictly as: Eq. (13):

$$C_{\text{optim}} = \underbrace{2}_{\text{Training Forward}} + \underbrace{4}_{\text{Training Backward}} = 6. \quad (13)$$

**Total Baseline and Data Selection Savings.** Cumulatively, the theoretical cost baseline per token scales with  $C_{\text{total}} = C_{\text{infer}} + C_{\text{optim}} = 10$ . For a global dataset  $D$  and epoch count  $E$ , the baseline expense is given by Eq. (14):

$$\text{FLOPs}_{\text{base}} \approx 10 \cdot E \cdot |D| \cdot n_{\text{rollout}} \cdot P \cdot T. \quad (14)$$

Our learning-zone data filtering regimen dynamically selects and retains only the prime 40% of sample groups mapping backpropagation. Generative inferences and objective energy scorings remain necessarily fully evaluated. The modified compute footprint explicitly rescales the optimization term, yielding Eq. (15):

$$\text{FLOPs}_{\text{ours}} \approx (C_{\text{infer}} + 0.4 \cdot C_{\text{optim}}) \cdot E \cdot |D| \cdot n_{\text{rollout}} \cdot P \cdot T = (4 + 0.4 \cdot 6) \cdot (\dots) = 6.4 \cdot (\dots). \quad (15)$$

Consequently, the structural computation conserved corresponds firmly to Eq. (16):

$$\text{Saved FLOPs} = 1 - \frac{6.4}{10} = 36\%. \quad (16)$$

This exact reduction isolates and eliminates redundant backward passes across uninformative state manifolds (fully-saturated or intrinsically out-of-distribution regimes), drastically widening practical scaling capabilities without compromising policy alignment limits.

## F Additional Ablation Studies

**Impact of Rollout Count  $N$ : Unconstrained Upper Bound.** Section 4.2 (Figure 3b) evaluates the effect of rollout count under a *fixed total rollout budget* of  $7.8 \times 10^5$ . Here we remove the budget constraint and instead run each  $N$  configuration for a fixed number of gradient steps (equal training iterations), so each experiment receives a different but unconstrained compute allocation. This measures the quality upper bound achievable by LZE at each  $N$  independently of cost.

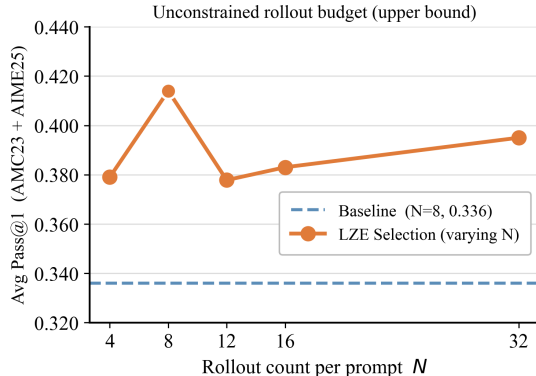


Figure 5: Rollout- $N$  sensitivity under an *unconstrained* budget. Each  $N$  runs for the same number of gradient steps; compute cost scales with  $N$ . Even under unconstrained conditions, LZE selection consistently outperforms the baseline at every  $N$ , and  $N=8$  again achieves the best absolute performance.

As shown in Figure 5, the qualitative pattern mirrors the fixed-budget result: LZE selection outperforms the full-data baseline at every rollout count, and performance peaks at  $N=8$  (Avg Pass@1 = 0.414 vs. baseline 0.336). Smaller  $N$  ( $= 4$ ) yields noisier group-level pass-rate estimates, making the Energy Score less reliable; larger  $N$  ( $\geq 12$ ) provides more stable estimates but offers diminishing returns—the gain from additional rollouts within a single step is small compared to the benefit of more gradient steps using the same compute. Together, the fixed-budget and unconstrained results confirm that  $N=8$  is a robust default across both efficiency-constrained and quality-maximising regimes.

**Sensitivity to the Momentum Coefficient  $\alpha$ .** The momentum term  $(1 + \alpha m_i^{(t)})$  in the Energy Score amplifies prompts where the pass rate is actively improving, with  $\alpha = 0$  reducing the score to a

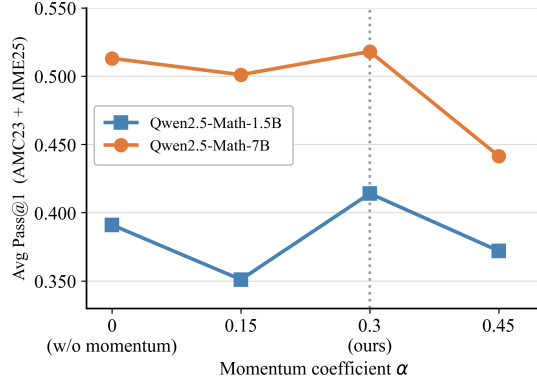


Figure 6: Sensitivity to the momentum coefficient  $\alpha$ . Both 1.5B and 7B models show consistent peaks at  $\alpha = 0.3$  (our default). At  $\alpha = 0$  the momentum term is absent; at  $\alpha = 0.45$  the score becomes overly reactive, destabilising selection.

purely uncertainty-based criterion (no momentum). We sweep  $\alpha \in \{0, 0.15, 0.3, 0.45\}$  on MATH with Qwen2.5-Math-1.5B and Qwen2.5-Math-7B, reporting  $\text{Avg Pass@1} = (\text{AMC23} + \text{AIME25}) / 2$ .

Figure 6 reveals a consistent non-monotone pattern across both model scales. Setting  $\alpha = 0$  (no momentum) already yields strong performance—confirming that the uncertainty term is the primary driver—but the momentum signal provides a meaningful further boost at  $\alpha = 0.3$ :  $+0.023$  for 1.5B ( $0.391 \rightarrow 0.414$ ) and  $+0.005$  for 7B ( $0.513 \rightarrow 0.518$ ). A smaller  $\alpha = 0.15$  under-utilises the temporal change signal and falls below the no-momentum baseline for the 1.5B model, suggesting that weak momentum can transiently mislead selection before the EMA has time to smooth out. An excessively large  $\alpha = 0.45$  makes the score overly sensitive to single-step fluctuations in the pass rate: transient improvements are over-rewarded, causing the selector to repeatedly re-select prompts that exhibited one lucky run but have not yet stably improved, which degrades the training distribution and reduces final accuracy. The sweet spot at  $\alpha = 0.3$  strikes the best balance between responsiveness and stability across both model sizes, and we adopt it as the default for all experiments in the main paper.

## G Use of LLMs

The drafting of this manuscript was enhanced through the use of a large language model, assisting in grammatical refinement.

## H Broader Impacts

The potential negative social impacts of our method are minor, and align with those typically associated with general LLM reasoning technologies. We emphasise the importance of adhering to the principles of fair and safe deployment of LLM systems, including careful consideration of the training data, transparency about model capabilities and limitations, and ongoing monitoring for unintended consequences.